

High-resolution scanning tunneling and atomic force microscopy of stereochemically resolved dibenzo[a,h]thianthrene molecules

Niko Pavliček¹, Coral Herranz-Lancho², Benoit Fleury², Mathias Neu¹, Judith Niedenführ¹, Mario Ruben^{*,2,3}, and Jascha Repp^{**1}

¹ Institute of Experimental and Applied Physics, University of Regensburg, 93053 Regensburg, Germany

² Institute of Nanotechnology (INT), Karlsruhe Institute of Technology (KIT), 76344 Eggenstein-Leopoldshafen, Germany

³ Institut de Physique et Chimie des Matériaux de Strasbourg (IMCMS), CNRS-Université de Strasbourg, 67034 Strasbourg, France

Received 21 May 2013, revised 17 July 2013, accepted 18 July 2013

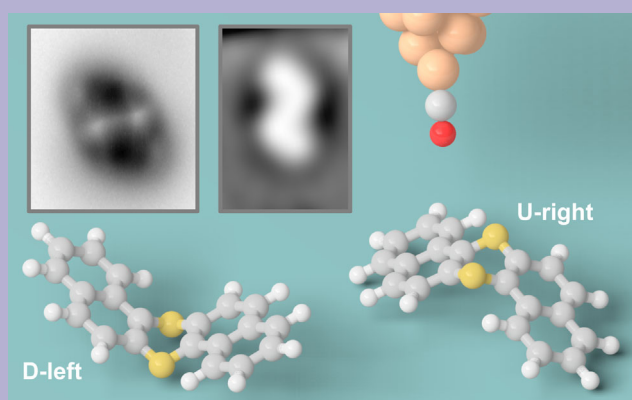
Published online 12 August 2013

Keywords charge density, contrast mechanisms, scanning probe microscopy, thianthrene

* e-mail mario.ruben@kit.edu, Phone: +49 721 60826781, Fax: +49 721 60826434

** Corresponding author: e-mail jascha.repp@ur.de, Phone: +49 941 9434201, Fax: +49 941 9432754

Recently, we reported on the bistable configurational switching of dibenzo[a,h]thianthrene (DBTH) molecules adsorbed on NaCl using combined low-temperature scanning tunneling and atomic force microscopy (STM/AFM). Here, we discuss the intra-molecular contrast in AFM images of the molecules as a function of the tip–molecule distance. Our experiments show that ridges in the frequency shift do not necessarily correlate with chemical bonds in this case of a non-planar molecule. To explain this finding we compare images acquired at different tip–molecule distances to the calculated electron density of the molecules obtained from density functional theory calculations (DFT). In addition, we analyze the probability of finding different configurations after adsorption onto the surface.



DBTH molecules in two configurations probed by a CO-functionalized tip. Insets show AFM (left) and STM (right) images of a U molecule.

© 2013 WILEY-VCH Verlag GmbH & Co. KGaA, Weinheim

1 Introduction By means of scanning tunneling microscopy (STM) it is possible to investigate electron transport through adsorbates and adsorbate structures in a large variety of aspects, while having exact knowledge and control of the atomistic structure including the coupling to the leads. Therefore, STM has been very successfully applied in the field of molecular electronics (for recent examples, see e.g., Refs. [1–3]). However, STM investigations are limited to conducting substrates and the experimental data is determined by both the geometry and the electronic structure of the sample in a complex and often ambiguous manner.

In recent years, the so-called frequency modulation mode [4] of atomic force microscopy (AFM) has advanced dramatically. As the qPlus sensor [5] does not require optical methods for sensing, it can be implemented in experimental setups working at the temperature of liquid helium with reasonable effort. In addition, it offers the application of combined STM and AFM with a usual STM tip, as the qPlus sensors can be mounted with conventional W or PtIr tips that are most widely used in standard STM setups. This combination of excellent stability at low temperatures and the combined STM/AFM capability has enabled a couple of

outstanding recent results. For example, the chemical structure of individual molecules [6–8] and the directionality of atomic bonds [9] could be resolved with sub-atomic resolution. In the field of molecular electronics, the interplay of force and current has been studied in various aspects [10–12]. It has enabled a force-controlled lifting of molecular wires while measuring their conductance [13], and the local electric field above an individual molecule has been resolved [14].

In the context of molecular switching, the combined STM/AFM approach allowed us to initiate switching in the STM channel, while observing the geometrical changes upon switching in the AFM channel [15]. In this example, the molecular switches consisted of individual dibenzo[a,h]thianthrene (DBTH) molecules. These molecules are within the family of thianthrenes, in which, due to the presence of the lone pairs of the thioether groups, the molecules are folded along the sulfur–sulfur (S–S) axis [16–23]. For a given orientation of the S–S axis, the molecule is bistable with respect to the folding angle. In solution it is not possible to resolve the stereochemistry of thianthrenes because the two enantiomers constantly interconvert into each other [24]. At the temperature of our experiments, the interconversion is frozen. Due to interactions with the substrate, the degeneracy of the different folding configurations will be lifted upon adsorption. To be able to observe both configurations, we wanted to keep these interactions low. This was achieved by adsorbing the molecules onto a weakly interacting surface, namely on ultrathin insulating layers of NaCl [25]. The use of ultrathin insulating films enables a measurable tunneling current to flow between tip and sample and thus allows for complementary STM measurements [26]. With this experimental setup we found DBTH molecules in different configurations. Two pairs of enantiomers with different appearances could be identified. For each of the pairs the two enantiomers differ in their chirality [28] and are connected by a mirror operation. In contrast, the different pairs of enantiomers cannot be interconverted into each other by means of any symmetry operation. Whereas these different species could be distinguished in STM [27], determining their geometry was only possible by means of the AFM data [15] – see Fig. 1. They correspond to a folding geometry with either upward- or downward-pointing sulfur atoms, as is depicted in Fig. 2. The existence of different enantiomers allowed us to also identify the interconversion pathway upon switching [29, 30].

Here we discuss additional results that are not covered in Ref. [15]. After introducing the methods, including the synthesis of the molecules in Section 2, we will describe the intra-molecular contrast of the molecules for larger distances in the force channel (Section 3). The latter findings we will discuss in relation to the calculated electron density of the molecules as obtained from density functional theory (DFT) calculations, presented in Section 4. The probability of finding different configurations after adsorption onto the surface is discussed in Section 5 before concluding the article.

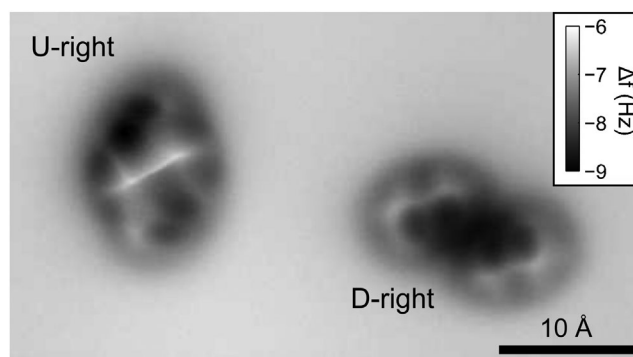


Figure 1 Constant height AFM imaging of DBTH in U and D configuration. Imaging parameters: oscillation amplitude $A = 0.6 \text{ \AA}$, $V = 0 \text{ V}$, $\Delta z = -0.3 \text{ \AA}$. Δz corresponds to a distance decrease with respect to an STM set point of $I = 0.5 \text{ pA}$, $V = 0.3 \text{ V}$ above the clean NaCl(2ML)/Cu(111).

2 Methods All AFM measurements were carried out in a homebuilt combined STM and AFM operating in an ultra-high vacuum ($p < 10^{-10} \text{ mbar}$) at $T = 5 \text{ K}$. The AFM, based on the qPlus tuning fork design (spring constant $k_0 \approx 1.8 \times 10^3 \text{ N m}^{-1}$, resonance frequency $f_0 = 26057 \text{ Hz}$, quality factor $Q \approx 10^4$) [31], was operated in the frequency modulation mode [4]. Sub-Ångstrom oscillation amplitudes have been used to maximize the lateral resolution [5]. Some of the STM measurements were performed in a similar modified commercial STM from SPS-CreaTec. The bias voltage V was applied to the sample.

Sodium chloride was evaporated onto clean Cu(111) single-crystals at sample temperatures of about 280 K [25]. All experiments were carried out on two or three layers

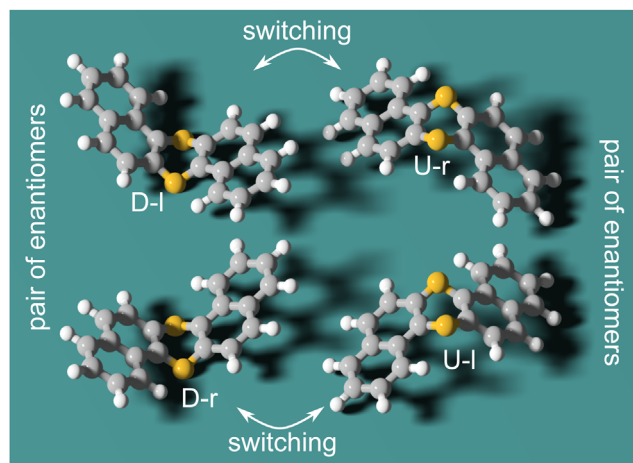


Figure 2 Illustration of all four possible configurations of DBTH on a homogeneous surface. White, gray, and yellow spheres represent H, C, and S atoms. There exist two pairs of enantiomers with the sulfur atoms pointing towards (D) and away from (U) the surface. For each of these pairs, the two enantiomers are left or right-handed, which we define with respect to the internal molecular structure disregarding the surface.

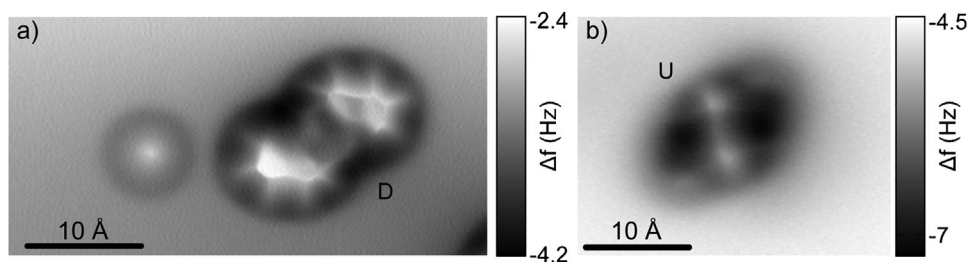


Figure 3 Constant height AFM imaging at different distances. (a) D molecule at closer tip–molecule distance as compared to Fig. 1. The molecule is adsorbed close to a CO molecule. At this distance the S atoms are also visible for D molecules. Imaging parameters: oscillation amplitude $A = 0.6 \text{ \AA}$, $V = 0 \text{ V}$, $\Delta z = -0.4 \text{ \AA}$. Δz corresponds to a distance decrease with respect to an STM set point of $I = 1.5 \text{ pA}$, $V = 0.3 \text{ V}$ above the clean NaCl(2ML)/Cu(111). (b) When imaging U molecules at larger tip–molecule distances, no apparent distortions due to bending of the CO molecule at the tip apex are visible ($A = 0.5 \text{ \AA}$, $V = 0 \text{ V}$, $\Delta z = -0.3 \text{ \AA}$ relating to $I = 0.5 \text{ pA}$, $V = 0.4 \text{ V}$).

of NaCl(100). Low coverages of CO (for tip functionalization) and DBTH molecules were adsorbed at sample temperatures below 10 K. Following a recently developed technique, the tip had been terminated with a CO molecule for all AFM measurements to enhance the resolution considerably [6].

To complement the experiments we have performed DFT calculations [32, 33] for a free DBTH molecule (that is, without substrate) using the highly optimized CPMD code [34], as described earlier in Ref. [15]. The cell size was $18 \text{ \AA} \times 16.2 \text{ \AA} \times 9 \text{ \AA}$, Perdew–Burke–Ernzerhof (PBE) exchange correlation functionals [35] and *ab initio* norm-conserving pseudo-potentials [36] were applied. The molecular structure has been found by minimizing the total energy and relaxing the ions until the forces on all atoms were below $5 \times 10^{-4} E_h/a_0$ ($\approx 40 \text{ pN} \approx 2.1 \text{ meV \AA}^{-1}$).

The DBTH molecules were synthesized in a two-step procedure from naphthalene-2-thiol [37]. First, oxidation of the thiol group to a disulfur-bridged specie is achieved quantitatively with hydrogen peroxide in the presence of sodium iodide. This intermediate has been described to rearrange in a good yield to DBTH by reaction with molybdenum pentachloride and titanium tetrachloride. The final compound was sublimed twice in order to enhance its purity.

3 AFM imaging In Ref. [15], AFM imaging was used to unambiguously identify the different configurations. The characteristics of the images were not discussed in detail. The vertical position Δz of the imaging plane for the constant height image shown in Fig. 1 has been chosen in such a way that both molecules could be resolved in the same image. However, for the imaging conditions used in Fig. 1, D molecules show moderate contrast, whereas the appearance of the U molecules is already quite distorted. These distortions have been previously attributed to a bending of the CO molecule at the CO-functionalized tip apex [38]. The distortion is particularly strong along the S–S axis. For U configurations the sulfur atoms stick out towards the tip, and the distortions are expected to be strongest there.

To investigate the intra-molecular contrast in more detail, we imaged a D (U) molecule at a tip–sample distance which was $\approx 0.45 \text{ \AA}$ smaller ($\approx 0.21 \text{ \AA}$ larger)¹ as compared to the imaging conditions of Fig. 1. These images are shown in Fig. 3. The image of the D molecule at a smaller distance also shows some intra-molecular resolution at the central part pointing towards the surface, whereas the upper part becomes more distorted—as is expected. The image of the U molecule at a larger distance shows less distortions. However, along the S–S axis, a ridge of the Δf -signal is still clearly visible, even though the image does not show strong distortions. In other cases, such ridges indicated molecular bonds [6, 7], but in the present case there should not be a bond between the sulfur atoms. This raises the question as to what causes the ridge of the Δf -signal along the S–S axis. This will be discussed further in the next section.

4 Density functional theory simulations In conjunction with our experiments, DFT calculations of individual DBTH molecules have been performed [15]. These calculations verified the initial assumptions of the bent molecular geometry. Furthermore, the calculations provided numbers for the relevant energy scales and electron densities that can be qualitatively compared to Δf -AFM images.

As a first step, we have optimized the structure by relaxing all atoms. As expected, we found the folded configuration to be the most stable one, having a folding angle of about

¹The relative differences in tip–sample distance were estimated as follows:

(i) To account for differences in the set-point current I , a decay constant $\kappa = 1 \text{ \AA}^{-1}$ for the current was used:

$$I(z) \propto \exp(-2\kappa z). \quad (1)$$

(ii) To account for differences in the oscillation amplitude A , the average current $\langle I \rangle$ was estimated using the relationship proposed in Ref. [39]:

$$\langle I \rangle(z, A) \propto \exp(-2\kappa z) J_0(2\kappa A), \quad (2)$$

where J_0 is the modified Bessel function of the first kind. (iii) Differences in the set-point bias voltage were accounted for by extrapolating the current in accordance with the linear $I(V)$ characteristics in this voltage range.

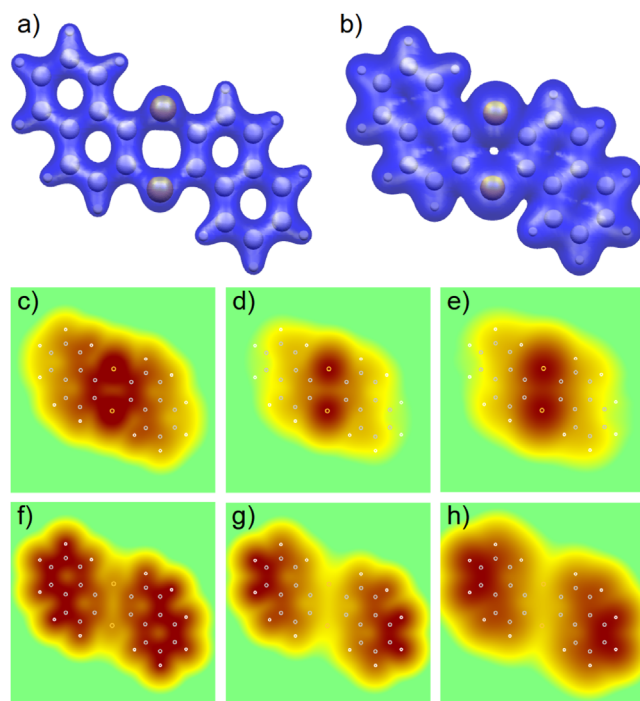


Figure 4 Illustration of the total charge density of DBTH molecules. (a and b) show three-dimensional isocontours for two different values of total charge density of a U molecule. (c–e) [f–h] show two-dimensional cuts of the total charge densities of a U [D] molecule along a plane being 0.5, 1.5, and 2.5 Å [1.5, 2.5, and 3.5 Å] above the sulfur atoms, respectively. The color scale is a logarithmic representation of the density and spans 4 orders of magnitude in density. Each frame is $15.9 \times 15.9 \text{ \AA}^2$. White, gray, and yellow circles indicate the positions of H, C, and S atoms.

$\Theta = 133^\circ$ [15]. This value is larger than the one observed for thianthrene by X-ray crystallography with $\Theta = 128^\circ$ [19], whereby the difference can be attributed to the extension of the π -conjugation in DBTH molecules, which tends to flatten the molecule. This effect can also be seen qualitatively in the atomic relaxations inside DBTH. The local bond angle for the S atoms is roughly the same as for thianthrene. However, the overall shape of the molecule is flattened, which is accomplished by a bending of the molecular structure over the length of two C–C bonds adjacent to the sulfur atoms, see side view in Fig. 5.

To gain insight into the energy barrier for flapping between both configurations, we have calculated the energy for different folding angles [15]. To this end, we have optimized the geometry for fixed angles ranging from 90° to 183° . That is, the atoms may relax with the constraint that the folding angle, as defined in Fig. 5, is fixed. Figure 5 shows that the energy barrier for flapping is approximately 200 meV. As expected, the relative energy diverges for very small ϕ , and is the same for 183° and 177° .

Finally, we return to the question of the contrast mechanism in Δf -AFM imaging. In Section 3, we have seen that for U molecules even at slightly larger distances the constant height Δf -images show a ridge-like feature along the S–S

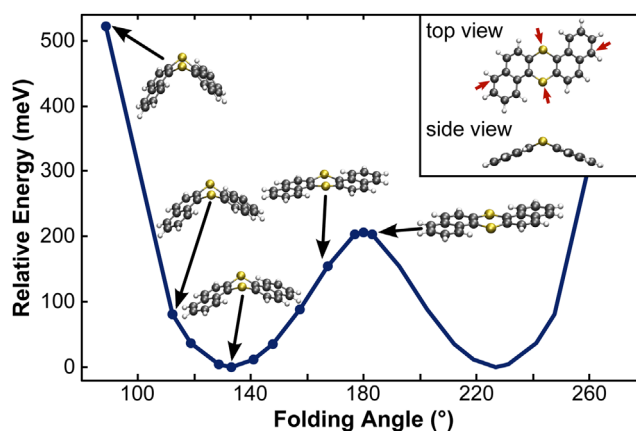


Figure 5 Relative energy of DBTH molecules as a function of folding angle ϕ . The total energy for the optimized geometry is set as zero. The curve has been mirrored with respect to a folding angle ϕ of 180° . The circles correspond to calculated energies in the illustrated geometries. White, gray, and yellow spheres represent H, C, and S atoms. The inset shows the relaxed geometry in top and side view. Red arrows in the top view model of DBTH indicate the atoms used to define the angle ϕ .

axis although there is no bond. Moll and co-workers [38] have shown that the intra-molecular contrast in constant-height Δf -images with CO-functionalized tips is dominated by Pauli-repulsion. The force contribution that is due to Pauli-repulsion is a monotonic function of the total electron density of the sample [38]. We therefore discuss the latter quantity in more detail here. Figure 4 shows various illustrations of the total charge density resulting from the DFT calculations. When plotting three-dimensional isosurfaces of this quantity, there is no enhanced charge density visible along the S–S axis. To more closely mimic the situation of a constant height image, Fig. 4 shows plots of the charge density in a two-dimensional plane that would be parallel to the surface for the adsorbed U configuration and that are 0.5, 1.5, and 2.5 Å above the sulfur atoms. For completeness, we also show plots for the D configuration that are 1.5, 2.5, and 3.5 Å above the sulfur atoms. To visualize the density despite its large variations, a logarithmic color scale has been used. The plots of the U configuration nicely reproduce the very high charge density at the positions of the sulfurs for all distances. This provides a possible explanation as to why U molecules show much stronger Δf -contrast and distortions than D molecules at the same imaging parameters. For the close distance, the contrast on the naphthalene units bares a resemblance to the image contrast in corresponding Δf -images at close distances [15]. The density slab that is 2.5 Å above the sulfur atoms shows just the high density at the sulfurs, which is smeared out laterally, such that also along the S–S axis the density is indeed higher than elsewhere. In conjunction with the finite size and bending of CO at the tip, this may be the reason for the ridge-like feature in the experimental images. This analysis shows that the presence or absence of bonds in the case of non-planar molecules apparently cannot always

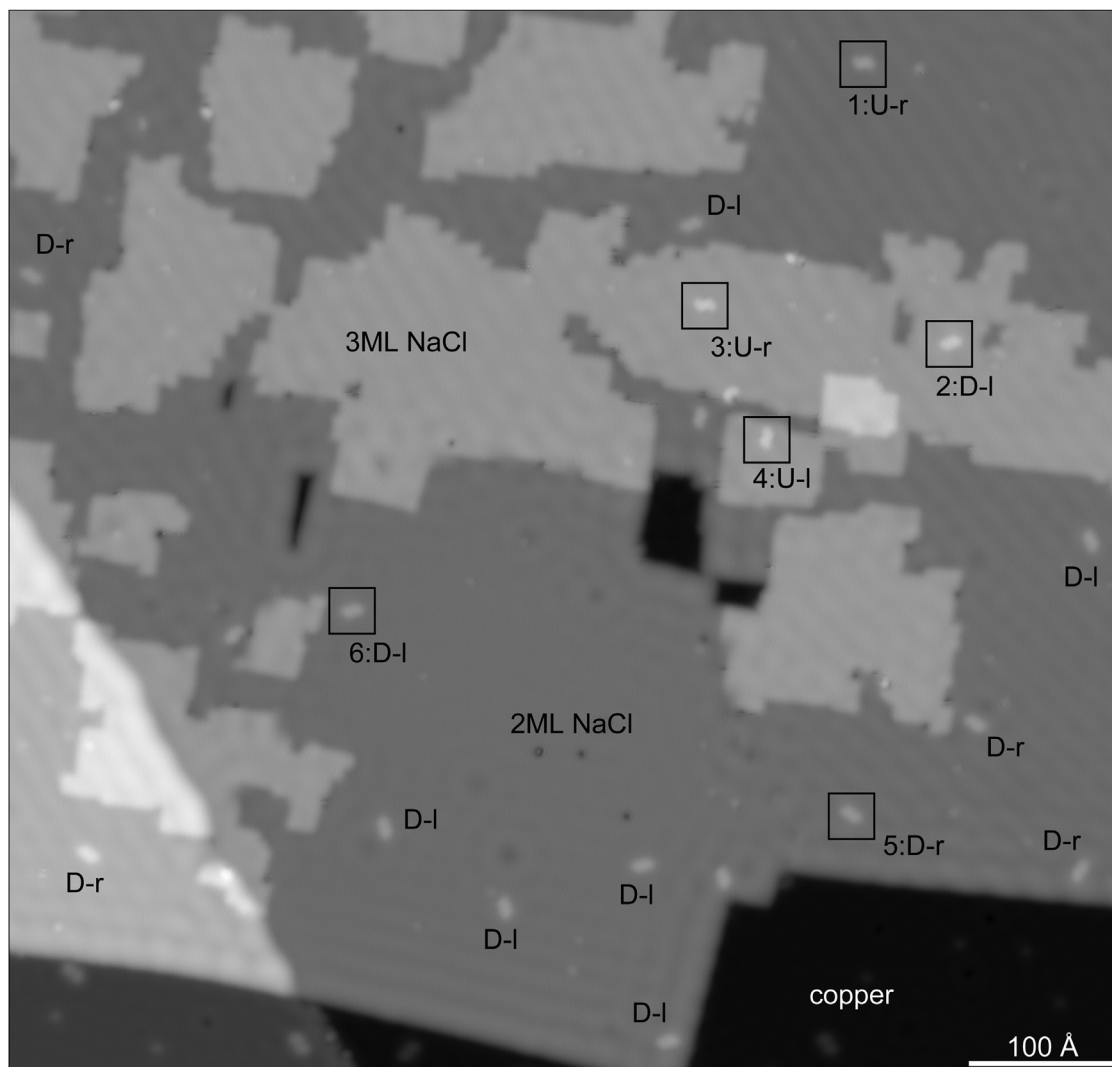


Figure 6 Overview STM image of DBTH molecules in different configurations on NaCl/Cu(111). Upon zooming in, the different configurations can be distinguished. The assignment to the configurations can be done from the combined STM/AFM results as reported in Ref. [15]. The configurations are indicated as U and D for up and down, respectively, as well as l and r for left-handed and right-handed, respectively. Details of the molecules marked with squares and labelled by numbers are shown in Fig. 7. Set point of $I = 0.4$ pA, $V = 0.05$ V.

be deduced just from looking at constant-height Δf -images. We hope that these observations will trigger further theoretical investigations on the imaging mechanism discussed here.

5 Configurations of as-adsorbed molecules The two configurations, with respect to the folding angle and the handedness of the molecules, result in four distinguishable geometries of the adsorbed molecules. Here, we follow the notation as was used in Ref. [15], namely U and D for upward- and downward-pointing sulfur atoms, and left- and right-handed depending on the chirality of the free molecule (cf. Fig. 2, as well as Fig. 3 of Ref. [15]).

The AFM data, as shown in Fig. 1, allows one to unambiguously assign the molecular configuration to one of the four possibilities. Knowing the configuration from the AFM data, one can also assign the slightly different appearances in the STM data to the four configurations, which allows one to discriminate them from STM images alone. Figure 6 shows a large-scale overview image of many individual DBTH molecules on the NaCl(100)/Cu(111) sample. The number of NaCl layers varies within the image from 0 to 3 and is indicated. The individual molecules were identified from their appearances as U-l, U-r, D-l, and D-r, where l and r denote the left- and right-handed enantiomers, respectively. The clear distinction is only possible in detailed views of the molecule, which are shown in Fig. 7 for six different molecules marked

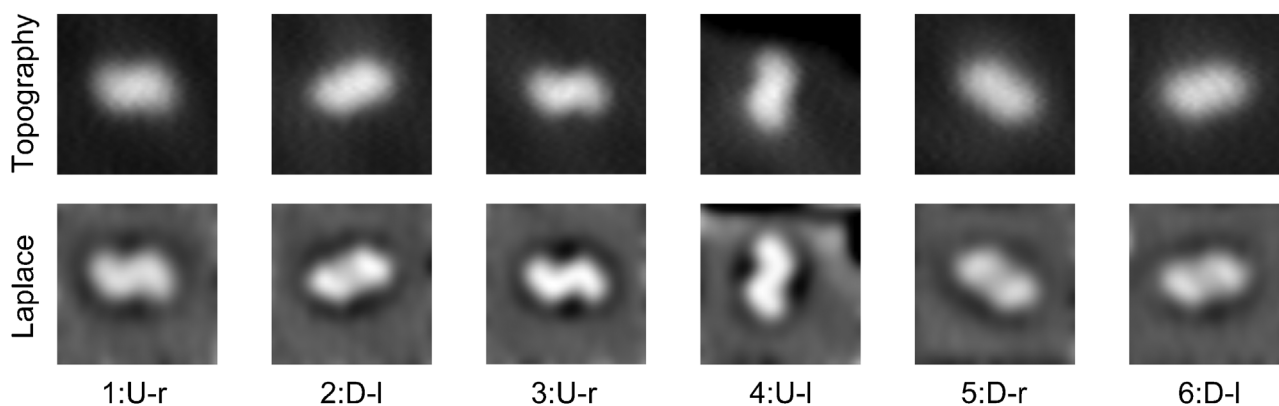


Figure 7 Detailed views of selected molecules from Fig. 6. The upper row are topographs, the lower row shows the same images after application of a high-pass filter (Laplacian). U and D configurations can be distinguished from the more (U) or less (D) pronounced s-shape of its image contour. l and r can be discriminated from the handedness of its s-shape appearance. Each frame is $30 \times 30 \text{ \AA}^2$.

in Fig. 6 as examples. Interestingly, U-l and D-r molecules exhibit a different image contour, despite the fact that their structure projected onto the surface plane is identical.

The same holds true for U-r and D-l molecules. U molecules show a much more pronounced s-shape of its image contour than D molecules. The chirality of the s-shape can be directly assigned to left- and right-handedness. Note that the handedness is defined with respect to the free molecules and not with respect to the projection of their structure to the surface plane.

In general, the images of molecules adsorbed on three layers of NaCl(100) exhibit a slightly stronger contrast (molecules 2, 3, and 4 in Fig. 7) than those adsorbed on two layers of NaCl(100) (molecules 1, 5, and 6 in Fig. 7). Within our limited sample of a couple of tens of molecules we find l and r molecules with equal probability. In the gas phase at room temperature and above, the two enantiomers constantly interconvert into each other as the energy barrier is only about 200 meV. Even if adsorbed on the surface, each two differently handed enantiomers corresponding to either U or D are degenerate, such that the adsorption process itself should not favour one of the two enantiomers. Hence, the equal probability of handedness after adsorption is expected.

This is different for the probabilities of finding molecules adsorbed in U and D configurations. Here we experimentally find only about every fourth molecule in U and the rest in D configuration. There may be two different reasons for this non-equal ratio. Firstly, this preference can arise if the solid angle of molecular orientations that lead to a certain adsorption configuration, i.e., U versus D, is different for the two. Hence, the v-shape geometry itself may already lead to a higher probability of landing on the surface with the angle pointing down (∇) than pointing up (\wedge). Secondly, U and D configurations will not be degenerate in adsorption energy, since for D the sulfur atoms interact with the sample surface, whereas for U hydrogen atoms are exposed towards the surface. As the molecules have a large kinetic energy in the moment of adsorption, the system might relax towards

the adsorption geometry with lower energy upon adsorption, even if afterwards both states are stable at low temperatures.

6 Conclusions The existence of four different stereoisomers of DBTH upon adsorption at surfaces was shown, whereby the relative stereochemistry of each isomer could be unambiguously determined from constant-height Δf -AFM images. The intra-molecular contrast of these images has been discussed and related to the total electron density as derived from DFT calculations. This revealed that the presence of ridge-like contrast features in the experimental images is not always indicative of a bond in the case of non-planar molecules.

Acknowledgements The authors thank Nikolaj Moll, Thilo Glatzel, and Franz J. Giessibl for valuable comments. Financial support from the Deutsche Forschungsgemeinschaft through the priority program 1243 is gratefully acknowledged.

References

- [1] Y. F. Wang, J. Kröger, R. Berndt, H. Vázquez, M. Brandbyge, and M. Paulsson, *Phys. Rev. Lett.* **104**, 176802 (2010).
- [2] G. Schull, T. Frederiksen, A. Arnau, D. Sánchez-Portal, and R. Berndt, *Nature Nanotechnol.* **6**, 23 (2011).
- [3] S. Schmaus, A. Bagrets, Y. Nahas, T. K. Yamada, A. Bork, M. Bowen, E. Beaupaire, F. Evers, and W. Wulfhekel, *Nature Nanotechnol.* **6**, 185 (2011).
- [4] T. R. Albrecht, P. Grütter, D. Horne, and D. Rugar, *J. Appl. Phys.* **69**, 668 (1991).
- [5] F. J. Giessibl, *Rev. Mod. Phys.* **75**, 949 (2003).
- [6] L. Gross, F. Mohn, N. Moll, P. Liljeroth, and G. Meyer, *Science* **325**, 1110 (2009).
- [7] L. Gross, F. Mohn, N. Moll, G. Meyer, R. Ebel, W. M. Abdel-Mageed, and M. Jaspars, *Nature Chem.* **2**, 821 (2010).
- [8] L. Gross, *Nature Chem.* **3**, 273 (2011).
- [9] J. Welker and F.-J. Giessibl, *Science* **336**, 444 (2012).
- [10] M. Ternes, C. González, C. P. Lutz, P. Hapala, F. J. Giessibl, P. Jelínek, and A. J. Heinrich *Phys. Rev. Lett.* **106**, 016802 (2011).
- [11] N. Hauptmann, F. Mohn, L. Gross, G. Meyer, T. Frederiksen, and R. Berndt, *New J. Phys.* **14**, 073032 (2012).

- [12] C. Lotze, M. Corso, K. J. Franke, F. von Oppen, and J. I. Pascual, *Science* **338**, 779 (2012).
- [13] N. Fournier, C. Wagner, C. Weiss, R. Temirov, and F. S. Tautz, *Phys. Rev. B* **84**, 035435 (2011).
- [14] F. Mohn, L. Gross, N. Moll, and G. Meyer, *Nature Nanotechnol.* **7**, 227 (2012).
- [15] N. Pavliček, B. Fleury, M. Neu, J. Niedenfuehr, C. Herranz-Lancho, M. Ruben, and J. Repp, *Phys. Rev. Lett.* **108**, 086101 (2012).
- [16] K. Fries, W. Volk, *Ber. Dtsch. Chem. Ges.* **42**, 1170 (1909).
- [17] L. E. Sutton and G. C. Hampson, *Trans. Faraday Soc.* **31**, 945 (1935).
- [18] I. Rowe and B. Post, *Acta Crystallogr.* **11**, 372 (1958).
- [19] H. Lynton and E. G. Cox, *J. Chem. Soc.* 4886 (1956).
- [20] J. Stenhouse, *Justus Liebigs Ann. Chem.* **149**, 247 (1869).
- [21] M. J. Aroney, R. J. W. Le Fèvre, and J. D. Saxby, *J. Chem. Soc.* 571 (1965).
- [22] K. L. Gallaher and S. H. Bauer, *J. Chem. Soc. Faraday Trans. 2* **71**, 1173 (1975).
- [23] S. Hosoya, *Acta Crystallogr.* **16**, 310 (1963).
- [24] G. H. Keats, *J. Chem. Soc.* 1592 (1937).
- [25] R. Bennewitz, V. Barwich, M. Bammerlin, C. Loppacher, M. Guggisberg, A. Baratoff, E. Meyer, and H.-J. Güntherodt, *Surf. Sci.* **438**, 289 (1999).
- [26] J. Repp, G. Meyer, S. M. Stojković, A. Gourdon, and C. Joachim, *Phys. Rev. Lett.* **94**, 026803 (2005).
- [27] T. A. Jung, R. R. Schlittler, and J. K. Gimzewski, *Nature* **386**, 696 (1997).
- [28] K.-H. Ernst, *Phys. Status Solidi B* **249**, 2057 (2012).
- [29] R. Raval, *Chem. Soc. Rev.* **38**, 707 (2009).
- [30] M. J. Comstock, D. A. Strubbe, L. Berbil-Bautista, N. Levy, J. Cho, D. Poulsen, J. M. J. Fréchet, S. G. Louie, and M. F. Crommie, *Phys. Rev. Lett.* **104**, 178301 (2010).
- [31] F. J. Giessibl, *Appl. Phys. Lett.* **76**, 1470 (2000).
- [32] P. Hohenberg and W. Kohn, *Phys. Rev.* **136**, B864 (1964).
- [33] W. Kohn and L. J. Sham, *Phys. Rev.* **140**, A1133 (1965).
- [34] CPMD V3.15 Copyright IBM Corp 1990–2011, Copyright MPI fuer Festkoerperforschung Stuttgart 1997–2001.
- [35] J. P. Perdew, K. Burke, and M. Ernzerhof, *Phys. Rev. Lett.* **77**, 3865 (1996).
- [36] D. R. Hamann, *Phys. Rev. B* **40**, 2980 (1989).
- [37] A. Spurg, G. Schnakenburg, and S. R. Waldvogel, *Chem. Eur. J.* **15**, 13313 (2009).
- [38] N. Moll, L. Gross, F. Mohn, A. Curioni, and G. Meyer, *New J. Phys.* **12**, 125020 (2010).
- [39] N. Berdunov, A. J. Pollard, and P. H. Beton, *Appl. Phys. Lett.* **94**, 043110 (2009).